Hindawi
Wireless Communications and Mobile Computing
Volume 2022, Article ID 6404493, 8 pages
https://doi.org/10.1155/2022/6404493

Research Article

The Effect of 3D Image Virtual Reconstruction Based on Visual Communication

Li Xu,[1] Ling Bai,[2] and Lei Li[3]

[1]*School of Art and Design, East University of Heilongjiang, Harbin 150001, China*
[2]*School of Information, Guangsha College, Harbin 150025, China*
[3]*International Department, Heilongjiang International University, Harbin 150025, China*

Correspondence should be addressed to Lei Li; lilei@hiu.edu.cn

Received 4 November 2021; Accepted 11 December 2021; Published 5 January 2022

Academic Editor: Alireza Souri

Considering the problems of poor effect, long reconstruction time, large mean square error (MSE), low signal-to-noise ratio (SNR), and structural similarity index (SSIM) of traditional methods in three-dimensional (3D) image virtual reconstruction, the effect of 3D image virtual reconstruction based on visual communication is proposed. Using the distribution set of 3D image visual communication feature points, the feature point components of 3D image virtual reconstruction are obtained. By iterating the 3D image visual communication information, the features of 3D image virtual reconstruction in visual communication are decomposed, and the 3D image visual communication model is constructed. Based on the calculation of the difference of 3D image texture feature points, the spatial position relationship of 3D image feature points after virtual reconstruction is calculated to complete the texture mapping of 3D image. The deep texture feature points of 3D image are extracted. According to the description coefficient of 3D image virtual reconstruction in visual communication, the virtual reconstruction results of 3D image are constrained. The virtual reconstruction algorithm of 3D image is designed to realize the virtual reconstruction of 3D image. The results show that when the number of samples is 200, the virtual reconstruction time of this paper method is 2.1 s, and the system running time is 5 s; the SNR of the virtual reconstruction is 35.5 db. The MSE of 3D image virtual reconstruction is 3%, and the SSIM of virtual reconstruction is 1.38%, which shows that this paper method can effectively improve the ability of 3D image virtual reconstruction.

1. Introduction

3D image virtual reconstruction technology has developed a set of stereo imaging system and has been gradually applied in various fields [1]. In recent years, with the continuous improvement of computer equipment and performance, virtual imaging technology has been well developed. In the traditional sense, 3D image virtual reconstruction technology uses computer technology to simulate the virtual environment and makes people feel the virtual environment or world through visual communication technology [2]. 3D image virtual reconstruction technology includes many disciplines and is a comprehensive composite virtual imaging technology, including computer modeling technology, virtual image processing technology, scene simulation technology, and human-computer interaction technology [3]. The effect of 3D image virtual reconstruction directly affects the overall visual and auditory experience of users. In the era of intelligence, 3D image virtual reconstruction technology is gradually widely used in military, education, medicine, and other fields. Using image processing technology and computer graphics technology to overlay texture image on the surface of a 3D scene geometric model, that is, texture mapping is an effective way to display the real world. Texture mapping technology integrates the best features of each method [4]. Texture mapping can greatly improve the visual richness of raster-scanned images with only a small amount of calculation. Texture mapping is one of the most successful new techniques in high-quality image synthesis [5]. Compared with traditional 2D images, 3D images have more visual impact, clear layers, and more bright colors. In the process of product development, it can better display the

development process and, at the same time, can support remote browsing, which saves users time and improves efficiency [6]. Visual communication technology can better convey information to users through visual media, instead of traditional 2D expressions. The new visual communication mode is adopted to infiltrate the information to be expressed into all aspects. The visual communication technology is applied to the virtual reconstruction of 3D image, the image processing is completed by computer, and the information to be expressed by the image is transmitted by visual symbols and expressed and transmitted to users through visual media [7].

Tereshchenko and Lysenko [8] put forward a medium analytical reconstruction method using proportional scattering, which can analytically reconstruct the medium under different parameters and analyze the scale coefficient and size of the object, which has better accuracy than the traditional analytical reconstruction method. Lee et al. [9] proposed a virtual database data recognition method based on a support vector machine. Through the collection and analysis of recognition scores of the periocular region, the training and evaluation of noisy iris are realized. The verification results of experiments show that this method has better robustness than the traditional method. Deabes and Bouazza [10] proposed a quantitative analysis and reconstruction method based on a locally integrated transform Kalman filter in order to realize the reconstruction of ECT system image. Through the error analysis of the collected image, a nonlinear system evaluation tool was constructed, and the authenticity and effectiveness of the method were verified through quantitative analysis. Wang et al. [11] put forward a 3D image reconstruction method using wireless domain truncation to solve the problems such as unsatisfactory reconstruction effect of small closed areas. Conformal transform is used for image reconstruction to optimize the image reconstruction information truncated in wireless domain. The results show that this method has higher accuracy for the reconstruction effect of small closed areas. In order to reconstruct the image information more accurately, Jiang et al. [12] used the infrared image reconstruction technology to measure the image information and construct the infrared image matrix equation. By solving the matrix equation, it is proved that this method has better reconstruction.

Based on the above research, this paper designs a 3D image virtual reconstruction method based on visual communication, so as to improve the effect of 3D image virtual reconstruction in visual communication. The main contributions of this paper are as follows: (1) Using the distribution set of 3D image visual communication feature points, the feature point components of 3D image virtual reconstruction are obtained. By iterating the 3D image visual communication information, the features of 3D image virtual reconstruction in visual communication are decomposed, and the 3D image visual communication model is constructed. (2) On the basis of calculating the difference of 3D image texture feature points, the spatial position relationship of 3D image feature points after virtual reconstruction is calculated, and the texture mapping of 3D image is completed. (3) According to the description coefficient of 3D image virtual reconstruction in visual communication, the results of 3D image virtual reconstruction are constrained by visual communication technology.

2. Design of 3D Image Virtual Reconstruction Method

2.1. 3D Image Visual Communication Model. In order to construct the visual communication model, the 3D image is reconstructed adaptively [13]. Assuming that the reconstructed image visually conveyed by the 3D image is S, the edge feature points of the original 3D image are extracted and expressed by (i, j). The texture gradient decomposition is performed on the extracted feature points; the distribution set of the feature points of the visual transmission of the 3D image is calculated, as shown in formula (1) [14].

$$w(i,j) = \frac{1}{Z(i)} \exp\left(-\frac{d(i,j)}{h^2}\right), \tag{1}$$

where $Z(i)$ is the first-order and gradient decomposition operator, and the calculation formula is as follows:

$$Z(i) = \sum_{j\in\Omega} \exp\left(-\frac{d(i,j)}{h^2}\right). \tag{2}$$

According to formula (2), 3D image is reconstructed at superresolution, and the distribution function of feature points is constructed [15]. With the help of visual communication, the virtual reconstruction of feature points is carried out for 3D image. Through the fusion of feature points, the decomposition of feature points of 3D image is realized, and the feature point component of 3D image virtual reconstruction is obtained as follows [16].

$$\min_c\left(\min_{y\in\Omega(x)}\left(\frac{I^c(y)}{A^c}\right)\right) = \tilde{t}(x)\,\min_c\left(\min_{y\in\Omega(x)}\left(\frac{J^c(y)}{A^c}\right)\right) + \left(1-\tilde{t}(x)\right), \tag{3}$$

where the fitting parameter of 3D image visual communication information is $\tilde{t}(x)$, and the feature vector of 3D image visual communication information is A^c. Assuming that $J(x)t(x)$ is the visual transmission coefficient, the iterative formula for visually conveying information in 3D images is [17]

$$\mathrm{bnr}_\beta(X) = R_\beta X - R_\beta X_1. \tag{4}$$

Assuming that the number of feature points of 3D image visual communication is $M \cdot N$, the 3D image is virtually reconstructed, and the feature decomposition formula of 3D image virtual reconstruction in visual communication is obtained as follows [18]:

$$\beta_i = \exp\left(-\frac{|x_i - x_j|^2}{2\sigma^2}\right)\frac{1}{\mathrm{dist}(x_i, x_j)}. \tag{5}$$

Combined with the decomposition of feature vector in formula (5), the detection of feature points of 3D image is realized, and the construction of the 3D image visual communication model is completed.

2.2. Texture Mapping of 3D Image. Suppose x_q is the eigenvalue of 3D image feature points, and y_q is the corresponding feature point in the corresponding virtual reconstructed image. In different spaces, the difference between 3D image texture feature points and virtual image texture feature points is z_q. Therefore, the difference calculation formula of 3D image texture feature points is obtained.

$$\delta = H\delta_0 - \left(\frac{m}{m}\right) C \sin(m), \tag{6}$$

where δ is the texture feature point difference, δ_0 is the initial 3D image, C is the number of texture feature points reconstructed from the 3D image, and m is the difference between the number of texture feature points of the 3D image in real and virtual space. Assuming that the number of texture feature points of the 3D image is m, then $y_q^2 = i\, m_q^2 j$. Substitute $y_q^2 = i m_q^2 j$ into formula (6) to obtain the following formula:

$$u(\delta, a, \beta) = \sum_{q=1}^{\infty} x_q \cos\left[y_q - \sqrt{\frac{y_q^2}{\delta}\left(\delta \cos p_q\right)} + z_q\right], \tag{7}$$

where $u(\delta, a, \beta)$ is the position function of virtual reconstruction feature points and q and p_q are the difference between feature points and area of virtual reconstruction, respectively. The wavelet function [19] is used to calculate the spatial position relationship of 3D image feature points after virtual reconstruction.

$$K = w(\delta, \beta) + \phi \cdot r(\delta, \beta) + u(\delta, \alpha, \beta), \tag{8}$$

where the pixel change rate and texture feature point transformation function of 3D image virtual reconstruction are $w(\delta, \beta)$ and $r(\delta, \beta)$, respectively, and ϕ is the texture feature point coordinates after reconstruction [20].

According to formula (8), the result of 3D image texture mapping can be obtained, that is,

$$S = K \cos(\delta_0 - a\beta), \tag{9}$$

where a is the position information of texture feature points after virtual reconstruction of 3D image and β is the mapping plane.

According to the above process, the texture mapping of 3D image is completed.

2.3. Reconstruction Algorithm of 3D Image Virtual Using Visual Communication. The training sample formula for obtaining 3D images and virtual reconstruction images x_{hi} by visual communication [21] is as follows:

$$X_{hi} = [x_{hi,1}, x_{hi,2}, \cdots, x_{hi,mn}]. \tag{10}$$

Assuming that it is the image result of virtual reconstruction of 3D image, quantitative analysis is performed, the auxiliary design of virtual image is completed, and the deep-seated texture feature points of 3D image are extracted, namely,

$$F_{hi} = \left[\text{Bhist}\left(T_{hi}^1\right), \cdots, \text{Bhist}\left(T_{hi}^{L_1}\right)\right]^T \in R^{(2L1)L_1 B}. \tag{11}$$

Through the visual communication technology, the extraction results of deep texture feature points of 3D image are obtained [22], namely,

$$F_{li} = \left[\text{Bhist}\left(T_{hi}^1\right), \cdots, \text{Bhist}\left(T_{hi}^{L_1}\right)\right]^T \in R^{(2L1)L_1 B}, \tag{12}$$

where the feature extraction results of 3D image feature points and virtual reconstructed feature points are F_{hi} and F_{li}, respectively. Bhist represents the design process of 3D image virtual reconstruction, and B represents the number of samples after texture decomposition.

Combined with the design method of visual communication technology, the training dictionary is constructed in *Sc SR*, and the complex feature dictionary samples D_h and D_1 of 3D image virtual reconstruction can be obtained. The feature points F_{hi} and F_{li} after reconstruction are extracted by K. The visual communication technology is used to compile it into the training dictionary [23], and the description coefficient of 3D image virtual reconstruction in visual communication is obtained as follows:

$$\{D_h, a\} = \text{argmin}\left|F_{hi} - D_h X_{hi} a\right|_2^2 + \sum_{i=1}^{K} \lambda_i \left|\alpha_i\right|_1, \tag{13}$$

$$\{D_1, a\} = \underset{D_1, a}{\text{argmin}}\left|F_{li} - D_1 X_{hi} a\right|_2^2 + \sum_{i=1}^{K} \lambda_i \left|\alpha_i\right|_1, \tag{14}$$

where $a = \{a_i\}_{i=1}^k$ is the deep learning auxiliary matrix, and λ_i represents the reconstructed virtual coefficient. If the original 3D image feature points and the reconstructed virtual image feature points are described in the same coding method, they are intensively trained through formula (15), and the calculation formula is

$$\{D_h, D_1, a\} = \underset{D_h, D_1, \alpha}{\text{argmin}} \frac{1}{N}\left|F_{hi} - D_h X_{hi} a\right|_2^2 + \frac{1}{M}\left|F_{li} - D_1 X_{hi} a\right|_2^2 + \left(\frac{1}{N} + \frac{1}{M}\right) \sum_{i=1}^{K} \lambda_i \left|\alpha_i\right|_1, \tag{15}$$

where N and M represent the feature point arrangement matrix and vector information in visual communication of 3D image virtual reconstruction, respectively. $1/N$ and $1/M$ use formula (13) and formula (14) for normalization processing; combined with visual communication technology,

the coding coefficient a_i of each 3D image feature point F_C and D_C is calculated and the coding matrix a is obtained. The dictionary is updated by a.

The constraint expression of 3D image virtual reconstruction result is

$$X^* = \text{argmin}_X |SHX - D_C Y|_2^2 + c|X - X_0|_2^2 + \gamma|(I - W)X|_2^2, \tag{16}$$

where S represents the sample information of the 3D image, H represents the virtual reconstruction image, $|X - X_0|_2^2$ represents the constraint information, and $(I - W)X|_2^2$ represents the virtual reconstruction constraint matrix of the 3D image. c and γ represent the feature point parameters after virtual reconstruction of the 3D image, respectively. W represents the weight matrix of the virtual reconstruction of the unit image. Through the constraints on the virtual reconstruction of the 3D image, the design of the virtual reconstruction algorithm for the 3D image is completed. The 3D image virtual reconstruction algorithm is shown in Figure 1.

According to Figure 1, firstly, the training samples of 3D image virtual reconstruction image are obtained, and the deep texture feature points of 3D image are extracted. Then, the training dictionary is constructed through visual communication technology to obtain the description coefficient of 3D image virtual reconstruction in visual communication. Then, the feature point arrangement matrix is obtained by centralized training, and the coding matrix is constructed to update the training dictionary. Finally, the constraints of image virtual reconstruction are determined to complete 3D image virtual reconstruction.

3. Experiments and Results

3.1. Data Description and Implementation Details. This paper uses the data set ScanNet to verify the effect of the 3D image virtual reconstruction method in visual communication. The ScanNet data set is an RGB-D video data set containing 2.5 million views in more than 1500 scans, annotated using 3D camera poses, surface reconstruction, and instance-level semantic segmentation (3D) reconstruction related. In this paper, 5000 images are used for training; 1000 images are used for testing. The number of pixels of 3D image is 16 $*$ 16; the 3D image size is 1200 mm $*$ 200 mm. Image definition is 2548 frames. The number of iterations is 10 times.

The evaluation indexes of this paper are as follows:

(1) Virtual reconstruction effect. The higher the resolution of 3D image, the clearer the edge of 3D image, indicating that the better the virtual reconstruction effect of 3D image, on the contrary, the worse the virtual reconstruction effect of 3D image

(2) Virtual reconstruction time. The longer the virtual reconstruction time, the lower the virtual reconstruction efficiency. On the contrary, the shorter the virtual reconstruction time, the higher the virtual reconstruction efficiency

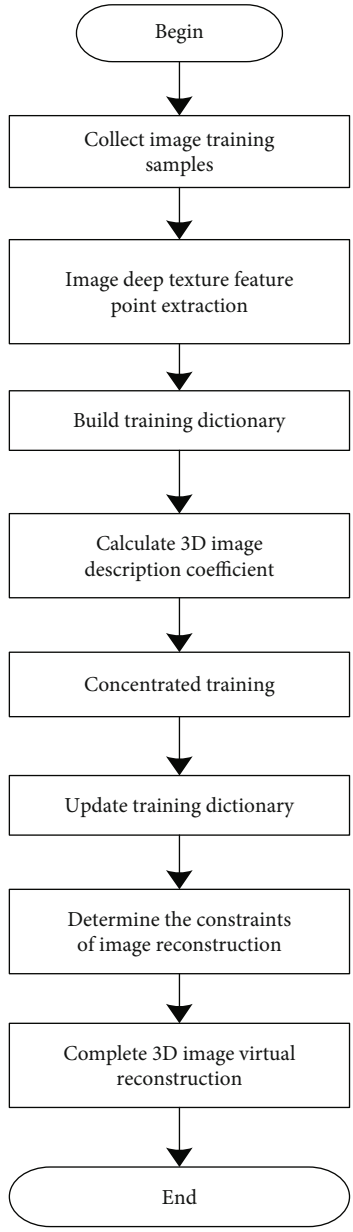

Figure 1: Algorithm process of 3D image virtual reconstruction.

(3) PSNR of 3D image reconstruction. The calculation formula is

$$\text{PSNR} = 20 \cdot \log_{10}\left(\frac{\text{MAX}_I}{\sqrt{\text{MSE}}}\right), \tag{17}$$

where MAX_I represents the color value of 3D image and MSE represents the MSE of virtual reconstruction. The higher the SNR ratio of 3D image reconstruction, the better the image quality. On the contrary, the lower the SNR ratio of 3D image reconstruction, the worse the image quality

(4) MSE of virtual reconstruction. The calculation formula is

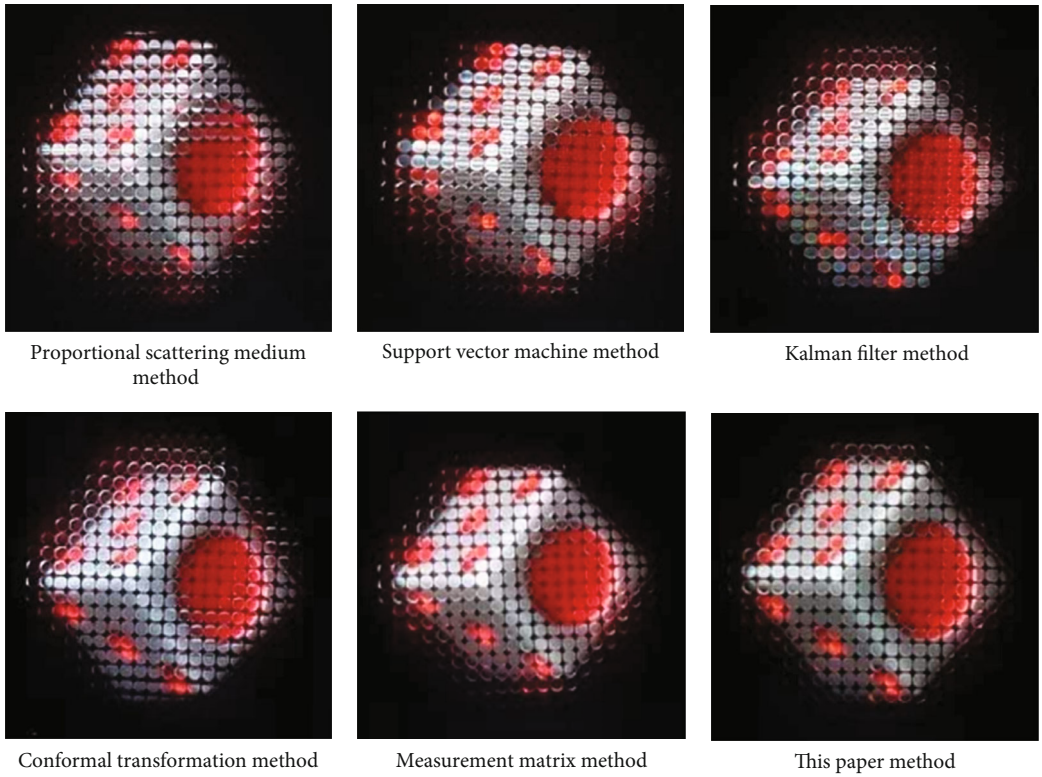

Figure 2: Virtual reconstruction effect of 3D image in visual communication.

$$\mathrm{MSE} = \frac{\sum_{i=1}^{r}(n_i - 1)s_i^2}{N - r}, \tag{18}$$

where $N - r$ is the freedom and $\sum_{i=1}^{r}(n_i - 1)$ is the sum of squares of reconstruction error. s_i^2 is the 3D image sample variance. The lower the virtual reconstruction MSE, the better the virtual reconstruction effect. On the contrary, the higher the virtual reconstruction MSE, the worse the virtual reconstruction effect

(5) SSIM of 3D image. The calculation formula is

$$\mathrm{SSIM}(x, y) = \frac{(2\mu_x\mu_x + c_1)(2\sigma_{xy} + c_2)}{\left(\mu_x^2 + \mu_y^2 + c_1\right)\left(\sigma_x^2 + \sigma_y^2 + c_2\right)}, \tag{19}$$

where x and y are the two 3D images. μ_x and μ_y are the average value of samples, σ_x and σ_y are the sample variance, and σ_{xy} is the covariance. The higher the SSIM of 3D images, the better the virtual reconstruction effect of 3D images in visual communication, on the contrary, the worse the virtual reconstruction effect

3.2. Results and Discussion. In order to highlight the advantages of the 3D image virtual reconstruction method in reconstruction, the reconstruction method based on proportional scattering medium [8], reconstruction method based on support vector machine [9], reconstruction method based on Kalman filter [10], reconstruction method based on conformal transformation [11], and reconstruction method based on measurement matrix [12] are introduced compared with the method in this paper. The following test results are obtained.

The virtual reconstruction effect of 3D image in visual communication is shown in Figure 2.

According to Figure 2, this paper method compared with the other five methods, the edge of the reconstructed 3D image of this paper method is clearer, the 3D effect is more obvious, and the resolution is relatively high, which has a better virtual reconstruction effect.

The test results of virtual reconstruction time of 3D image in visual communication are shown in Figure 3.

The results in Figure 3 show that when the number of samples is 200, the virtual reconstruction time of the proportional scattering medium method is 27 s, the virtual reconstruction time of the support vector machine method is 20 s, the virtual reconstruction time of the Kalman filter method is 14 s, the virtual reconstruction time of the conformal transformation method is 10 s, the virtual reconstruction time of measurement matrix method is 5.1 s, and the virtual reconstruction time of this paper method is 2.1 s. With the increase of the number of samples, the virtual reconstruction time of 3D images in visual communication is relatively close by using the measurement matrix method and the method in this paper, but the time used by this paper method is the shortest, within 3 s; other methods have poor performance in terms of virtual reconstruction time of 3D images.

The test result of the virtual reconstruction SNR of the 3D image in visual communication is shown in Figure 4.

The results in Figure 4 show that when the system running time is 5 s, the virtual reconstruction SNR of the

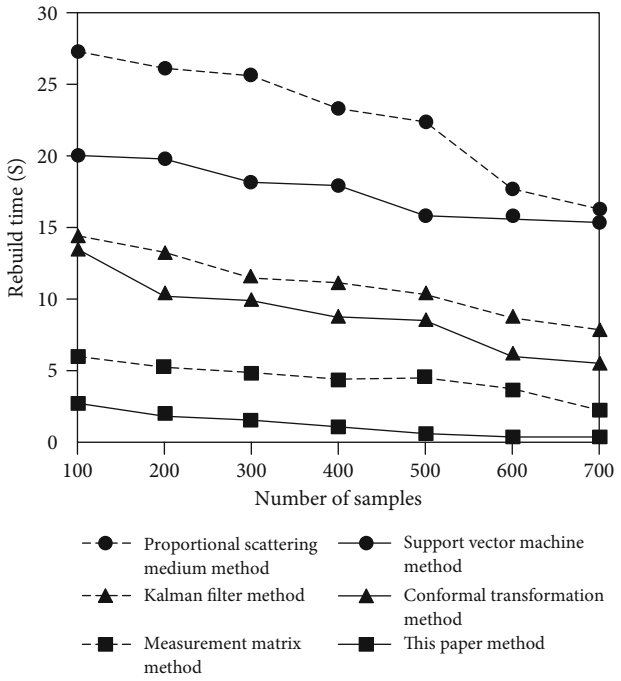

Figure 3: Virtual reconstruction time of 3D image in visual communication.

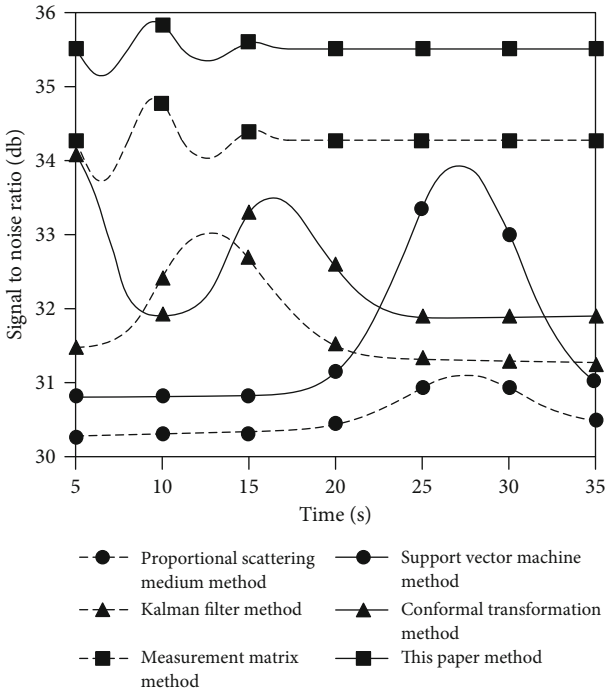

Figure 4: Virtual reconstruction SNR of 3D image in visual communication.

proportional scattering medium method is 30.2 db, the virtual reconstruction SNR of the support vector machine method is 30.9 db, the virtual reconstruction SNR of the Kalman filter method is 31.4 db, the virtual reconstruction SNR of the conformal transformation method is 34 dB, and

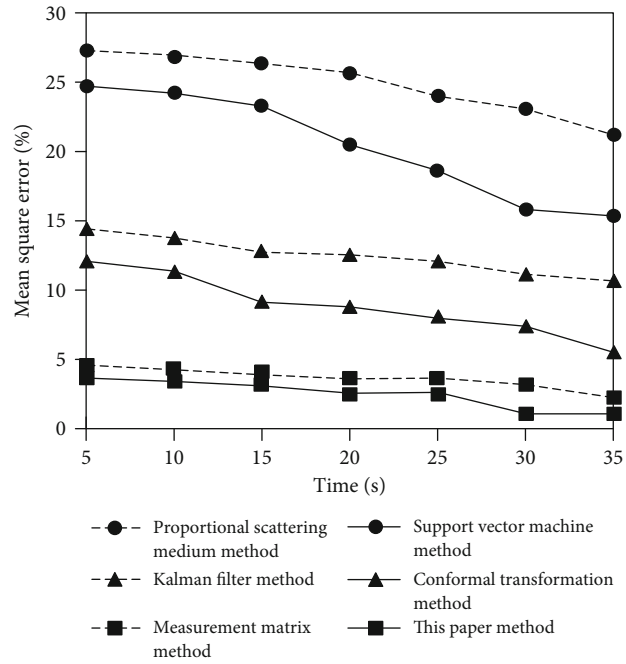

Figure 5: Virtual reconstruction MSE of 3D image in visual communication.

the virtual reconstruction SNR of the measurement matrix method is 34.2 db. The virtual reconstruction SNR of this paper method is 35.5 db. The SNR of 3D image virtual reconstruction obtained by the proportional scattering medium method, measurement matrix method, and this paper method is relatively stable, but the 3D image virtual reconstruction method can use visual communication technology to improve the SNR of 3D image virtual reconstruction and has better performance.

The test results of virtual reconstruction MSE of 3D image in visual communication are shown in Figure 5.

According to Figure 5, in terms of the MSE of virtual reconstruction of 3D image in visual communication, the results obtained by the proportional scattering medium method and support vector machine method exceed 15%, while the results obtained by the Kalman filter method and conformal transformation method are between 5% and 15%, which is difficult to realize the virtual reconstruction of 3D image. The results obtained by the measurement matrix method and this paper method are less than 5%, which can meet the requirements of 3D image virtual reconstruction, but the MSE obtained by this paper method is lower.

The SSIM of the virtual reconstruction results of 3D images in visual communication are shown in Figure 6.

It can be seen from Figure 6 that the change trend of 3D image virtual reconstruction SSIM of all methods is relatively close, but the method in this paper shows better performance in 3D image virtual reconstruction SSIM, which is more than 1.2%. Therefore, it is explained that this paper method can effectively improve the ability of 3D image virtual reconstruction.

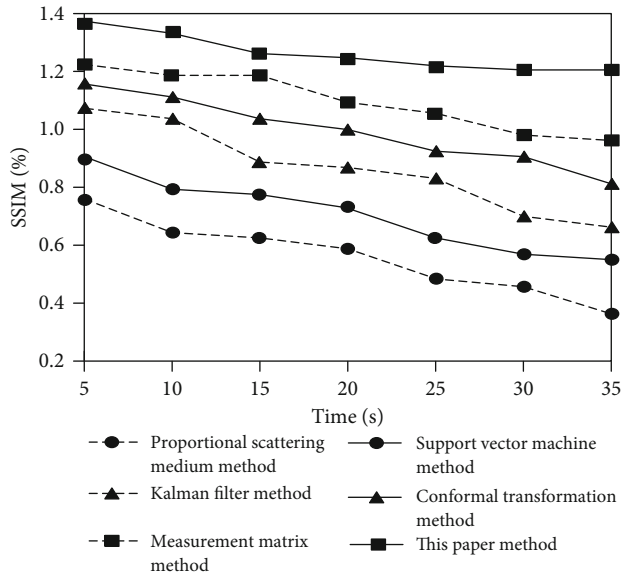

Figure 6: Virtual reconstruction SSIM of 3D image in visual communication.

4. Conclusions

This paper proposes the effect of 3D image virtual reconstruction in visual communication. By iterating the 3D image visual communication information, the features of 3D image virtual reconstruction in visual communication are decomposed, the 3D image visual communication model is constructed, and the spatial position relationship of 3D image feature points after virtual reconstruction is calculated. Through the visual communication of 3D image, the deep texture feature points of 3D image are extracted. According to the description coefficient of 3D image virtual reconstruction in visual communication, the virtual reconstruction results of 3D image are constrained by visual communication technology, and the virtual reconstruction algorithm of 3D image is designed to realize the virtual reconstruction of 3D image. The following conclusions are drawn through experiments: (1) When the number of samples is 200, the virtual reconstruction time of this paper method is 2.1 s, which shows that this paper method can effectively improve the virtual reconstruction efficiency. (2) When the system running time is 5 s, the virtual reconstruction SNR of this method is 35.5 db. The SNR of virtual reconstruction is high. (3) The MSE of 3D image virtual reconstruction obtained by this paper method is less than 5%, which can meet the requirements of 3D image virtual reconstruction. However, there are still many deficiencies in this paper. In the future work, we hope to analyze and screen the factors affecting 3D image virtual reconstruction and improve the efficiency of 3D image virtual reconstruction.

Data Availability

The data used to support the findings of this study are available from the corresponding author upon request.

Conflicts of Interest

The authors declare that there is no conflict of interest with any financial organizations regarding the material reported in this manuscript.

References

[1] X. Pan, Q. Zhao, and J. Liu, "Edge extraction and reconstruction of terahertz image using simulation evolutionary with the symmetric fourth order partial differential equation," *Optoelectronics Letters*, vol. 17, no. 3, pp. 187–192, 2021.

[2] W. Gao, A. Shakoor, M. Xie et al., "Precise automated intracellular delivery using a robotic cell microscope system with three-dimensional image reconstruction information," *IEEE/ASME Transactions on Mechatronics*, vol. 25, no. 6, pp. 2870–2881, 2020.

[3] A. Daoui, M. Yamni, O. El Ogri, H. Karmouni, M. Sayyouri, and H. Qjidaa, "Stable computation of higher order Charlier moments for signal and image reconstruction," *Information Sciences*, vol. 521, pp. 251–276, 2020.

[4] V. Frøysa, G. J. Berg, T. Eftestøl, L. Woie, and S. Ørn, "Texture-based probability mapping for automatic scar assessment in late gadolinium-enhanced cardiovascular magnetic resonance images," *European Journal of Radiology Open*, vol. 8, p. 100387, 2021.

[5] F. Tian, Y. Gao, Z. Fang, J. Gu, and S. Yang, "3D reconstruction with auto-selected keyframes based on depth completion correction and pose fusion," *Journal of Visual Communication and Image Representation*, vol. 79, p. 103199, 2021.

[6] H. Liu, W. Song, Y. Zhang, and A. Kudreyko, "Generalized Cauchy degradation model with long-range dependence and maximum Lyapunov exponent for remaining useful life," *EEE Transactions on Instrumentation and Measurement*, vol. 70, pp. 1–12, 2021.

[7] G. Fahim, K. Amin, and S. Zarif, "Single-view 3D reconstruction: a survey of deep learning methods," *Computers & Graphics*, vol. 94, pp. 164–190, 2021.

[8] S. A. Tereshchenko and A. Y. Lysenko, "Investigation of the scattering influence on the quality of image reconstruction in single-photon emission computed tomography in a proportional scattering medium," *Biomedical Engineering*, vol. 53, no. 5, pp. 370–374, 2020.

[9] M. B. Lee, J. K. Kang, H. S. Yoon, and K. R. Park, "Enhanced iris recognition method by generative adversarial network-based image reconstruction," *IEEE Access*, vol. 9, pp. 10120–10135, 2021.

[10] W. Deabes and K. E. Bouazza, "Efficient image reconstruction algorithm for ECT system using local ensemble transform Kalman filter," *IEEE Access*, vol. 9, pp. 12779–12790, 2021.

[11] Y. Wang, S. Ren, and F. Dong, "A transformation-domain image reconstruction method for open electrical impedance tomography based on conformal mapping," *IEEE Sensors Journal*, vol. 19, no. 5, pp. 1873–1883, 2019.

[12] Y. Jiang, H. Wang, R. Shao, and J. Zhang, "Infrared image reconstruction based on Archimedes spiral measurement matrix," *Journal of Shanghai Jiaotong University (Science)*, vol. 24, no. 2, pp. 204–208, 2019.

[13] N. Huang, Y. Ma, M. Zhang, H. Ge, and H. Wu, "Finite element modeling of human thorax based on MRI images for EIT image reconstruction," *Journal of Shanghai Jiaotong University (Science)*, vol. 26, no. 1, pp. 33–39, 2021.

[14] J. A. Fessler, "Optimization methods for magnetic resonance image reconstruction: key models and optimization algorithms," *IEEE Signal Processing Magazine*, vol. 37, no. 1, pp. 33–40, 2020.

[15] T. He and X. Li, "Image quality recognition technology based on deep learning," *Journal of Visual Communication and Image Representation*, vol. 65, article 102654, 2019.

[16] J. Zhang, Y. Gu, H. Tang et al., "Compressed sensing MR image reconstruction via a deep frequency-division network," *Neurocomputing*, vol. 384, pp. 346–355, 2020.

[17] S. K. HashemizadehKolowri, R.-R. Chen, G. Adluru et al., "Simultaneous multi-slice image reconstruction using regularized image domain split slice-GRAPPA for diffusion MRI," *Medical Image Analysis*, vol. 70, no. 2, article 102000, 2021.

[18] D. Połap and G. Srivastava, "Neural image reconstruction using a heuristic validation mechanism," *Neural Computing and Applications*, vol. 33, no. 17, pp. 10787–10797, 2021.

[19] X. Ma and X. Li, "Dynamic gesture contour feature extraction method using residual network transfer learning," *Wireless Communications and Mobile Computing*, vol. 2021, 11 pages, 2021.

[20] J. Huang, X. Liu, and Y. Lei, "X-ray phase-contrast image reconstruction based on the Chambolle-Pock algorithm," *Access*, vol. 9, pp. 23120–23126, 2021.

[21] A. Picon, A. Medela, L. F. Sanchez-Peralta et al., "Autofluorescence image reconstruction and virtual staining for in-vivo optical biopsying," *IEEE Access*, vol. 9, pp. 32081–32093, 2021.

[22] D. Liang, J. Cheng, Z. Ke, and L. Ying, "Deep magnetic resonance image reconstruction: inverse problems meet neural networks," *IEEE Signal Processing Magazine*, vol. 37, no. 1, pp. 141–151, 2020.

[23] D. Dan, Z. Wang, X. Zhou et al., "Rapid image reconstruction of structured illumination microscopy directly in the spatial domain," *IEEE Photonics Journal*, vol. 13, no. 1, pp. 1–11, 2021.